Effects of Selected Process Parameters on the Morphology of Poly(ethylene terephthalate) Preforms and Bottles

Tracey Hanley,[1,2] David Sutton,[1,2] Inna Karatchevtseva,[1,2] David Cookson,[2,3] Robert Burford,[1,4] Robert Knott[1,2]

[1]*Australian Nuclear Science and Technology Organisation, Private Mail Bag 1, Menai, New South Wales 2234, Australia*
[2]*Cooperative Research Centre for Polymers, 32 Business Park Drive, Notting Hill, Victoria 3168, Australia*
[3]*ChemMatCARS, Advanced Photon Source, Argonne, Illinois 60439*
[4]*School of Chemical Sciences and Engineering, University of New South Wales, Sydney, New South Wales 2052, Australia*

Received 18 September 2006; accepted 24 January 2007
DOI 10.1002/app.26472
Published online 19 June 2007 in Wiley InterScience (www.interscience.wiley.com).

ABSTRACT: Small-angle X-ray scattering (SAXS) studies and polarized optical microscopy were undertaken to explore possible morphological explanations for the poor mechanical strength in the petaloid bases of poly(ethylene terephthalate) bottles. With a standard commercial production line, one set of injection-molded preforms was overpacked by 1.1 wt % to investigate the effect on the molecular morphology with respect to a set of control samples. Both sets of preforms showed highly crystalline and oriented areas corresponding to the injection gate region. The main body of the control preform was amorphous, and although the overpacked preform was essentially amorphous, there was some evidence for weak crystallinity. The SAXS patterns of the bottle petaloid base blown from the corresponding preforms produced similar SAXS patterns for overpacked and control bottle bases, indicating that the commercial process is robust at least to this degree of overpacking. Optical microscopy showed detailed crystalline features around the gate region and thin crystalline layers sandwiched between a quenched skin layer in direct contact with the cold mold walls and the main flow of material into the mold. J Appl Polym Sci 106: 238–247, 2007

Key words: orientation; polyesters; SAXS

INTRODUCTION

Because of their mechanical stability and manufacturing efficiency, poly(ethylene terephthalate) (PET) bottles with petaloid bases are now widely used for liquid containers, particularly for carbonated soft drinks (CSDs). Bottles are manufactured by a two-stage injection–stretch–blow molding process that is highly automated and, in the main, well understood. In stage I, the PET bottle preforms [see Fig. 1(a)] are injection-molded in batches of around 96 and then rapidly cooled to room temperature. This results in a preform that is effectively amorphous, although the area of the polymer adjacent to the injection gate of the mold can be partially crystalline because of the proximity of the hot runner. In stage II, the preforms are reheated to a temperature above the glass transition but below the cold crystallization temperature and stretch–blow-molded into bottles of a given design. The crystallinity and molecular orientation induced by this two-stage process are essential to imparting the required mechanical properties (strength, optical clarity, etc.).[1–7] To manage this process in a commercial environment requires an enormous amount of knowledge that has been developed in this field over many years.

This petaloid base motif [Fig. 1(b)] is well established commercially; however, as design techniques develop, further research and development can be expected, particularly with computational methods used to predict the mechanical properties of complex shapes of polymeric materials.[8] Currently, research into improvements is in progress[9] with the aim of overcoming some of the known limitations of the petaloid design.

One existing limitation is circumferential cracking of the petaloid base, a well-known phenomenon for which the underlying causes are poorly understood.[10] A second limitation is a center crack that runs through, or close by, the gate [Fig. 1(b)]. The center crack is thought to be related to low-quality preforms or a poorly programmed stretch–blow

Correspondence to: T. Hanley (tracey.hanley@ansto.gov.au).
Contract grant sponsor: Australian Synchrotron Research Program; contract grant number: 03/04-CM-43.
Contract grant sponsor: National Science Foundation/Department of Energy; contract grant number: CHE0087817.
Contract grant sponsor: Illinois Board of Higher Education.
Contract grant sponsor: U.S. Department of Energy (through Basic Energy Sciences, Office of Science); contract grant number: W-31-109-Eng-38.

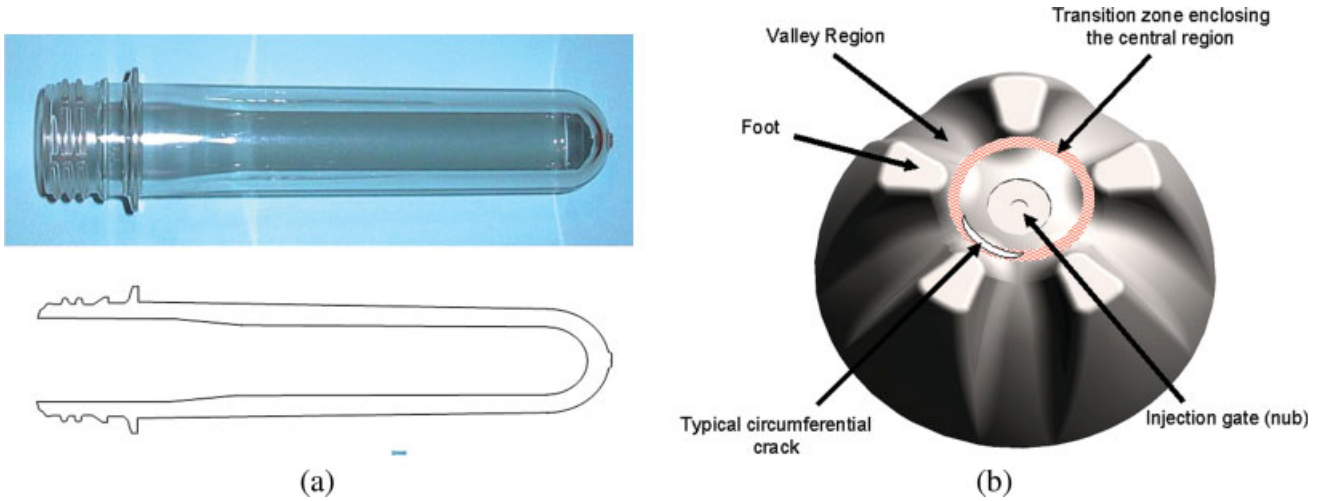

Figure 1 (a) Cross section of an injection-molded preform and (b) an engineering (rendered) drawing of a typical petaloid bottle base made by two-stage injection–stretch–blow molding from PET. [Color figure can be viewed in the online issue, which is available at www.interscience.wiley.com.]

molding phase.[10] As part of an extended research program on the molecular structure of PET,[11] small-angle X-ray scattering (SAXS) techniques have been developed to investigate the morphology of PET chains under a range of controlled experimental conditions (e.g., temperature, shear, and chain composition) that model industry conditions. These SAXS techniques have been used to explore the molecular organization of PET molecules in the petaloid bases of high-quality bottles and bottles that have split under a load.[12] The results indicate that different molecular morphologies do indeed exist, the details of which are discussed later.

SAXS is an ideal technique for exploring the molecular morphology of bulk polymers and has been used extensively to investigate the structure of PET under a variety of experimental conditions.[13–22] The typical wavelength of an angstrom or so enables a scattering vector ($\mathbf{q}$) range of $\sim 0.002 < \mathbf{q} < 0.4$ Å^{-1}, which corresponds to imaging on molecular length scales. Also, sample preparation is limited to the production of a ~1-mm-thick slice of material. Depending on the source of the X-ray used (synchrotron or laboratory), the X-ray beam can explore spatial variations from a few micrometers to a millimeter or so in a single SAXS pattern and can be readily scanned across a large area (millimeter to centimeter) of a sample to provide a comprehensive view of the molecular structure. These features made it the ideal technique to investigate the molecular structure of PET samples selected from a commercial production line.

Even given the extensive prior knowledge of the PET molecular structure, it is always advisable to use multiple experimental techniques when samples are investigated, particularly those prepared with a complex industrial process. In the past, we have used transmission electron microscopy;[23] however, we considered it inappropriate for this study because of the complex sample preparation (e.g., thin samples and staining) and the very small area scanned per image. Optical microscopy was considered more appropriate, having sufficient spatial resolution to provide supporting evidence for the molecular morphology distribution derived from the SAXS patterns.

The packing pressure of the injection-molded preform and the temperature of the preform during stretch–blow molding are considered to be important in determining the mechanical properties of the final blown bottle.[3] During the packing phase, the gate valve remains open, allowing more material to be forced into the mold cavity, and therefore an increased hold time will generally increase the final weight of the preform. The gate valve then closes to form the complete mold cavity. Because of the proximity of the hot runner system (used to deliver the molten PET into the mold), the gate valve has to be insulated to minimize the transfer of heat into the mold. Too much heat transfer would cause too much crystallinity in the gate region, making the region more susceptible to failure during and after bottle blowing. During the injection stage, the preform is also being cooled in preparation for removal from the mold. Therefore, a longer hold time implies that more material is forced into the end of the preform that ultimately forms the base of the bottle. More efficient cooling to the body and neck of the preform allows these regions in the mold to resist the addition of more material. In this study, the hold time was deliberately increased so that the effect of overpacking on the molecular morphology of the preform and bottles could be investigated.

Preform reheating for the stretch–blow molding phase also plays a significant role in defining the

ultimate performance of the bottle. Reheating is normally achieved with infrared radiation supplied by an array of lamps in conjunction with convection heating. The aim of the reheating process is to raise the temperature of the preform body into the range of 90–115°C. This range is high enough to avoid pearlescence (stress whitening due to microvoiding) but below the cold crystallization temperature that would produce haze in the bottle. Axial temperature profiling is controlled so that both ends of the preform remain cooler while the body reaches the ideal temperature. The neck above the support ring must remain cool to prevent distortion of the bottle closure region, whereas the bottom end of the preform must remain cooler to withstand the force of the stretch rod. The temperature profile along the body may vary to reflect any tapering in the thickness of the walls. Clearly, the temperature profiling at the base of the preform during the stretch–blow phase will make a major contribution to the final molecular morphology of the petaloid base. The likelihood of failure by cracking is directly related to the polymer chain morphology, so both phases of the production process can significantly influence cracking susceptibility.

A routine two-stage injection–stretch–blow molding process should lead to an amorphous region in the center of the bottle base (although the gate itself is semicrystalline). This central region is immediately followed by a biaxially oriented region in the feet and valleys, which progresses into the bottle wall. The residual stresses in the base material have been calculated with Abaqus simulation software,[9] and the stress calculations indicate maximum stress is present in the valley regions. Lyu et al.[24] used computer modeling to study crack formation in the base and concluded that cracks were formed in regions with inadequate strength. These low-strength regions resulted from areas in which strain hardening did not occur because of insufficient stretching of the polymer, basically as a result of a coarse base design. The base cracks also resulted from crazing that occurred because of the maximum principle stress being located in the valleys, and this crazing strongly affected the crack formation.

In a typical 2-L CSD bottle, the thickness of the PET in the walls is 0.35 ± 0.1 mm, whereas the thickness over the central region of the base is 2.1 ± 0.4 mm. In the transition region between the base center and either the foot or valley, the thickness is reduced as the material is stretched. A reduced thickness leads to a reduced strength of the base until the material is stretched far enough for strain hardening to occur, and at this point, there is a dramatic increase in the overall strength that compensates for the reduction in the thickness. Obviously, there remains a suspect region in which the material is thinning, but strain hardening and subsequent crystallization have yet to take place.[12]

Lyu and Kim[25] produced a further study that concluded that the key design parameters affecting circumferential cracking in the bottle base are the foot length, valley width, and clearance (the height difference between the gate position and the surface on which the bottle stands). Computer simulations were used to find the optimum values for design parameters that reduced the principle stress concentration, and these values were then used to design a new base that resulted in increased crack resistance.[9]

Our previous SAXS study[12] confirmed that the base center of good bottles was indeed amorphous. The circumferentially cracked bottles, however, exhibited a different morphology in the base center, in which the polymer chains were circumferentially aligned around the preform injection point. The SAXS results did not, however, identify any crystallinity within the central base region (aside from the gate as expected). This circumferential alignment produces an even weaker transition region, which is where the cracks are located. Our study concluded that the problem lies with either overpacking during preform injection or with temperature control of the preform base during the stretch–blow–molding phase.

For this study, no attempt was made to explore any skin/core effects of the bottle bases, although research by Everall et al.[26] indicated that skin/core effects are important. In a study using polarized attenuated total reflection FTIR spectroscopy on bottle walls,[26] complex orientation patterns and gradients were shown to exist in the skin/core regions that depend on the preform and mold design. It was shown that the differences in hoop extension for the inner and outer surfaces of a bottle wall are significant for the overall morphological properties. Typical values are ~5 and 4 for the inner and outer walls, respectively, of a 2-L bottle. The different geometry of the base means that there is unlikely to be any significant differences in hoop extension between inner and outer surfaces until the base starts to curve into the bottle wall, well beyond the transition region of interest. However, differences may exist because of rapid cooling of the skin during the injection-molding process, which freezes the skin while the core material is still flowing into the mold.

EXPERIMENTAL

The preforms and bottles were manufactured from commercial-grade PET (Skypet BL8050, SK Chemicals, Jakarta, Indonesia; intrinsic viscosity = 0.80 dL/g, melting temperature = 245°C, density = 1.40 g/cm^3) with a two-stage injection–stretch–blow molding process operating under standard industry conditions.

Before use, PET was thoroughly dried to a moisture content of ~25 ppm with a Novotec 1400 dryer (Merelbeke, Belgium). All the manifolds of the injection-molding machine (G-line 600 E140, Husky, Bolton, Canada) were set to a temperature of 290°C, and a balanced H-runner system (Husky) ensured that all molds were filled simultaneously. An insulated gate valve, which was heated for 45% of the cycle, formed the interface between the hot runner system and the mold. There was a maximum injection pressure of 2200 bar, and the hold pressure for the control samples consisted of three steps: 880 bar for 1 s, 900 bar for 2.5 s, and finally 930 bar for 3 s. For the overpacked samples, the hold time for step 1 was increased from 1 to 5.5 s. The total cycle time for the control samples was under 20 s, and this increased to just under 24.5 s for overpacked samples. A three-stage robotic cooling head was used to cool the injection-molded preforms. Stretch–blow molding was conducted with a Krones S24 machine (Neutraubling, Germany) operating under standard industry conditions.

The two sets of preforms and corresponding bottles blown from preforms, taken from the same mold positions, were collected. U-sections were cut from the injection end of the preforms [Fig. 1(a)] and carefully abraded to a thickness of 1.8 ± 0.2 mm. During cutting and abrading, the surface temperature remained well below the cold crystallization temperature for PET. The U-sections enabled SAXS data to be collected in the transmission mode through the thickness of the preforms, particularly around the injection gate. To complete the study, the petaloid bases were cut from the bottles to provide a clear path for the X-ray beam in the transmission mode. No other sample preparation was required.

Data were collected on the SAXS instrument on the ChemMatCARS 15-ID-D beam line (Advanced Photon Source, Chicago, IL).[27] A 500-μm-wide and 200-μm-high X-ray beam with a wavelength of 1.3 Å (9.54 keV) was selected. The two-dimensional (2D) SAXS patterns were collected with a Bruker 6000 CCD detector (Karlsruhe, Germany) (an active area of 94 × 94 mm^2 with a pixel size of 92 μm), which was located 1887 mm from the sample position. This geometry enabled a d-spacing in the range of 40–1100 Å (i.e., molecular dimensions) to be studied. The d-spacing was derived from Bragg's law ($\lambda = 2d \sin\theta$; where λ is the wavelength of the incident radiation and 2θ is the scattering angle) and is inversely related to $\mathbf{q}$ ($\mathbf{q} = 4\pi \sin\theta/\lambda$). $\mathbf{q}$ is, in turn, related to the position of the scattered X-ray on the 2D detector, with $\mathbf{q} = 0$ $Å^{-1}$ at the center of the detector. The total $\mathbf{q}$ range for the outlined instrument configuration was $0.007 < \mathbf{q} < 0.3$ $Å^{-1}$. A beam stop was located on a supporting arm to prevent permanent damage to the detector by the intense beam of X-rays. The intensity of the incident beam was estimated to be ~1×10^{12} photons per second.

The U-sections were mounted on an X–Y translation stage, and the software was programmed to collect data for 10 s before the stage was automatically moved to the next position. The U-sections were mounted with the injection point uppermost, and in the following discussions, the vertical direction (Y axis) was parallel to the wall of the preform, and the horizontal direction (X axis) was across the width of the preform. Standard SAXS data collection was as follows: In the horizontal direction, the X-ray beam was 500 μm wide, and 10 points were measured, spaced evenly over 10 mm of the sample. In the vertical direction, the X-ray beam was 200 μm high, and 20 points were measured, spaced evenly over 4 mm of the sample. This raster scanning regime mapped the gate area of the preform in detail, covering the region of the preform that ultimately formed the center of the petaloid bottle base, the zone susceptible to center cracks.

For the bottles, the petaloid base was mounted on the X–Y translation stage, and the beam was scanned vertically over the diameter of the base, covering 80 mm from one edge of the foot to the opposite edge of the valley. Data were collected for 10 s at 1-mm intervals across the base. The SAXS intensity was not placed on an absolute scale, and because the sample thickness varied over the base, the SAXS pattern was used to highlight qualitative differences in the crystallinity and orientation.

An Zeiss Axioplan optical microscope (Jena, Germany) fitted with polarization optics was subsequently used to record color images of the U-sections of the preforms in the transmission mode. Because of the thickness of the samples, crystalline regions appeared dark with respect to the amorphous regions of the samples.

RESULTS AND DISCUSSION

The average weight of the control preforms was 54.55 ± 0.07 g, whereas the weight of the overpacked preforms was 55.15 ± 0.07 g. The standard errors were calculated from a sample size of seven. Therefore, a 69% increase in the total hold time meant that the overpacked preforms were typically 1.1% heavier than the control preforms, and it was expected that most of this extra weight would be located around the gate region of the preform. Figures 2 and 3 show the mosaics of SAXS patterns for the control and overpacked preforms, respectively. The patterns are arranged immediately adjacent to one another in the mosaics to present a more compact figure and therefore do not reflect exactly the absolute position of each pattern on the preform, although they do represent the correct sequence. Pat-

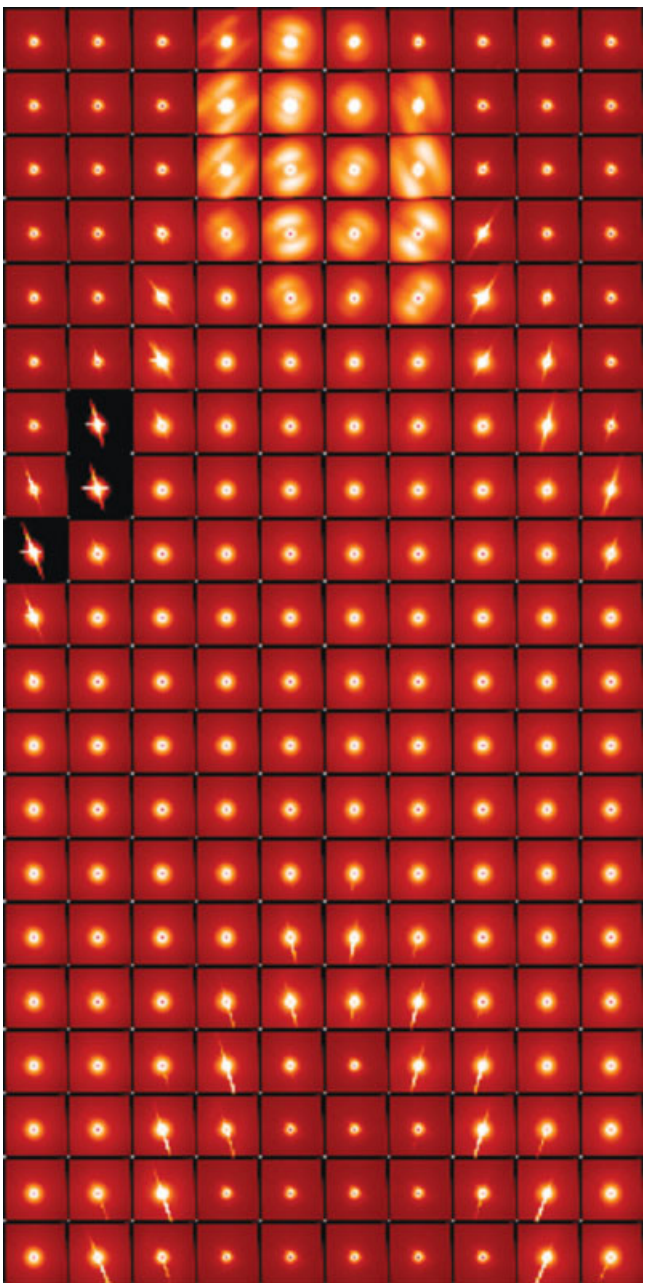

Figure 2 Mosaic of SAXS patterns collected from around the gate of a control preform. Horizontally, 10 patterns were collected over 10 mm; vertically, 20 patterns were collected over 4 mm. The beam size was 500 μm × 200 μm. In these 2D images, the color scale represents the number of X-rays collected per detector pixel. Bright areas indicate more intense scattering that merges into the darker background regions. The dark spot in the center of the image was caused by the beam stop. [Color figure can be viewed in the online issue, which is available at www.interscience.wiley.com.]

terns are all presented on a log intensity scale; they are geometrically corrected and are also normalized to the incident X-ray intensity. The color scale represents the number of X-rays detected in each pixel; bright colors represent high counts and dark colors represent low counts per pixel. The small dark region in the center of the SAXS pattern (see later figures) was caused by a beam stop located immediately in front of the detector to prevent the intense unscattered X-ray beam from causing damage to the detector.

Figures 2 and 3 contain a region of SAXS patterns located at the top and center of the mosaics that exhibit strong scattering. These regions correspond

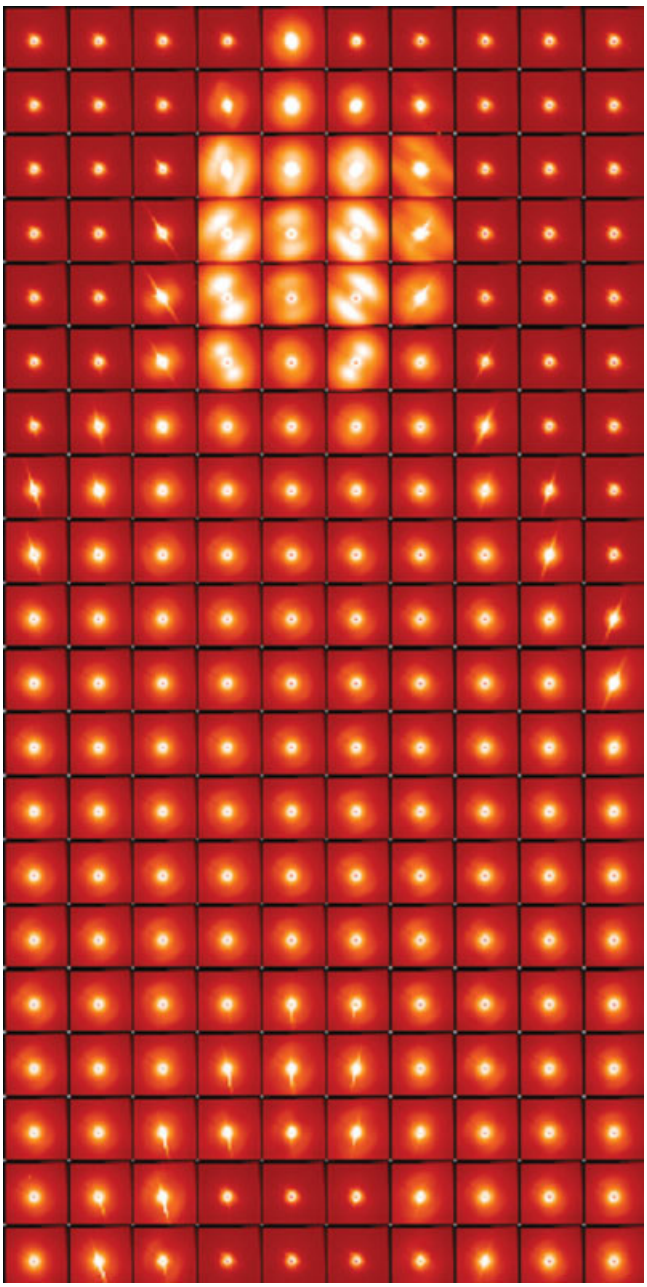

Figure 3 Mosaic of SAXS patterns collected from around the gate of a overpacked preform. Horizontally, 10 patterns were collected over 10 mm; vertically, 20 patterns were collected over 4 mm. The beam size was 500 μm × 200 μm. [Color figure can be viewed in the online issue, which is available at www.interscience.wiley.com.]

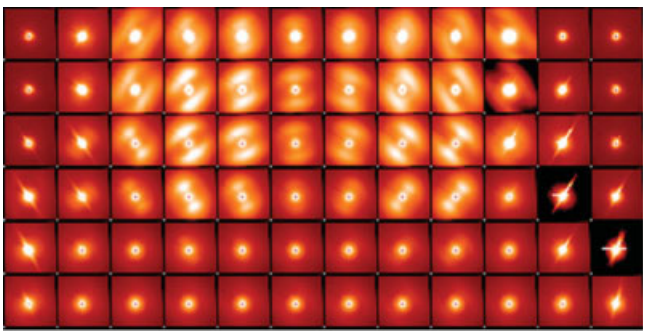

Figure 4 Mosaic of SAXS patterns collected from around the gate of an overpacked preform. Horizontally, 12 patterns collected were over 6 mm; vertically, 6 patterns were collected over 1.2 mm. The beam size was 500 μm × 200 μm. [Color figure can be viewed in the online issue, which is available at www.interscience.wiley.com.]

to the gate of the preforms at which the material is injected into the mold. On either side of the gate (upper left and right quadrants), there are (featureless) patterns due to air scatter only, and patterns containing only air scatter can also be seen at the bottom center of the mosaics. These air-scatter regions bound the shape of the inverted U-section. Some of the patterns contain intense streaks of scatter passing through the pattern center and are due to X-rays reflecting off the preform edge.

Figure 4 shows a mosaic of SAXS patterns from around the gate of another overpacked sample but with greater sampling in the horizontal scale, with 12 patterns taken over 6 mm (i.e., no gaps between the SAXS patterns). The vertical resolution in Figure 4 remains the same as that for Figures 2 and 3, although here only the top six rows are shown, covering a vertical distance of 1.2 mm. Again, air-scatter patterns are present in the top left-hand and right-hand quadrants of the mosaic. The enhanced horizontal sampling presents the gate structure in greater detail. The upper central patterns of the mosaic all show broad lobes located on either side of the direct beam, which are indicative of oriented lamellae. In the top three rows of the sixth column (counting from the left), the lobes of the scattered intensity are essentially aligned in a vertical axis, that is, above and below the direct beam. Previous model experiments that studied shear-induced crystallization have shown that this orientation is indicative of a flow direction approximately in the vertical direction, as would be expected from material flowing into the mold.[28] The crystalline lamellae orient perpendicularly to the flow direction in the horizontal direction, and the scattering from these lamellae forms the lobes above and below the direct beam.

All the lobes in the gate region are very broad at a constant **q**. Because SAXS patterns are in reciprocal space, broad lobes equates to shorter lamellae in the horizontal plane. Conversely, long lamellae (in the horizontal plane) would produce a much narrower lobe or spot in the vertical axis of the SAXS pattern. Hence, the broad lobes provide information about the local environment in the gate region, indicating that short lamellae develop that may be due to a restriction on space, possibly as a result of a high nucleation density caused by enhanced molecular alignment (see later). Still considering the sixth column in the mosaic of patterns, we find that the long axis of the polymer chains would be aligned in the vertical axis to form lamellae in the horizontal plane. This vertical alignment of the chains is almost certainly due to the shear forces experienced by the chains as they flow through the gate and into the mold. Areas of high shear are known to preferentially align polymer chains parallel to the flow direction, and this can lead to enhanced nucleation of crystals, especially where long chain polymers are present with slow relaxation times.[29]

In the top four rows of columns three to five and on the left of the central sixth column, the lobes have rotated in an anticlockwise direction with respect to the sixth column. Conversely, in columns seven to ten on the right-hand side of the central column, the lobes have rotated in a clockwise direction. This orientation of the lobes is directly related to the orientation of the lamellae in that region. A possible mechanism for the orientation of these lobes is discussed later after reference to the optical microscopy results. It may be useful to consider the local environment in more detail. After the packing phase, the gate valve closes to form the final part of the mold. To prevent melt crystallization in the valve, the valve is heated for 45% of the cycle time while the melt is flowing into the mold. Once it is inside the mold, the walls are cooled in an attempt to quench the PET into the amorphous state so that demolding can proceed as soon as possible. In fact, a quenched skin layer forms on immediate contact with the cold mold walls. The proximity of the hot runner system and heated valve in the gate region results in an area of a large thermal gradient. The valve itself is insulated from the mold in an attempt to minimize the degree of direct heating into the gate region, although enough heat is transferred so that cooling of the melt in the gate region is sufficiently slow to allow some crystallization.

Scattered lobes are virtually absent in row five of Figure 4. This is typical for all of the samples tested and roughly equates to a depth of 1 mm. The polymer chain morphology in the preform gate region, described in detail for Figure 4, is also applicable to the morphology observed for all the other samples examined at the standard lower data sampling rate with 10 SAXS patterns collected over 10 mm in the horizontal direction (Figs. 2 and 3 plus other data

not shown). It is also evident in Figure 4 that the scattering due to oriented lamellae down the central (sixth) column of the gate region is slightly less intense than that on the columns on either side and generally disappears about 200 μm (one row) before the adjacent columns. These observations were consistent for all the samples examined. This indicates that the degree of crystallinity in the central column of the gate is slightly less than that of the surrounding columns, suggesting that a ring of crystals may be present containing a central channel of slightly lower crystallinity.

With reference to Figure 2, it is apparent that the bulk of the control preform away from the gate is amorphous as intended. The preform patterns in Figure 3 appear brighter than the patterns in Figure 2; however, this was due to the overpacked preform section being slightly thicker and therefore having a greater number of scattering elements. After the contrast settings for the figures (patterns not shown) are enhanced, it is apparent that the overpacked sample exhibits very weak crystallinity and orientation over large regions of the preform. This weak effect could clearly be the result of overpacking, even though the gate regions for both sets of samples appear to be similar.

Figure 5 presents an example of a scan across the base of an overpacked bottle, taken from the same mold position as the preform shown in Figure 3. The sequence starts at the outer edge of the foot and passes over the foot, through the center, and through the valley directly opposite. All bottle bases were examined across two different axes (one foot apart) to check for uniformity. In fact, all the scans for both types of bases were virtually identical. The only differences occurred during the passage over the gate region, and this was due to the fact that not all the gates were located perfectly in the center of the bottle base. The first pattern (top left of Fig. 5) is from the outer edge of the foot, and the sequence continues row by row across the base until the final pattern bottom right at the outer edge of the valley. The top two rows correspond to 20 mm over the foot, whereas the bottom two rows correspond to 20 mm over the valley. The four oriented and crystalline patterns in rows four and five are due to the gate region. Figure 5 clearly shows that the regions over the foot and valley are crystalline, with some slight anisotropy at certain points, whereas the central region of the base, aside from the gate, is amorphous. This morphology is typical of a good bottle base. Clearly, the effort to create poor bottles by

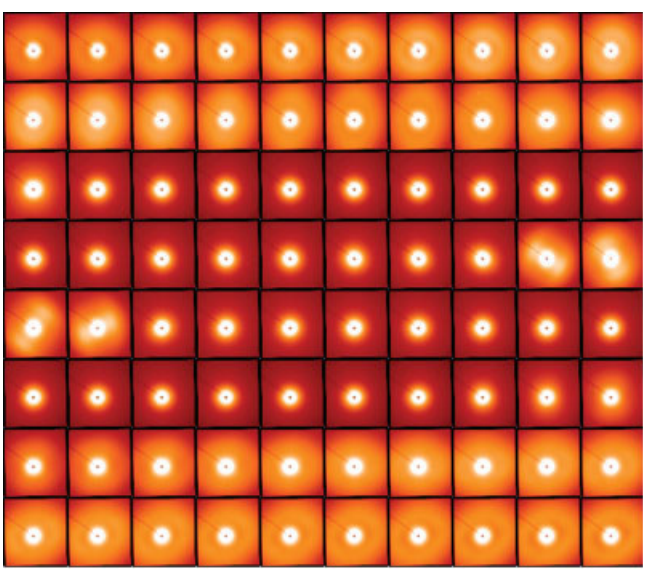

Figure 5 Sequence of SAXS patterns collected over the base of a 2-L CSD overpacked bottle, starting at the outer edge of the foot (top left) and passing over the foot, through the center, and over the valley opposite (bottom right). [Color figure can be viewed in the online issue, which is available at www.interscience.wiley.com.]

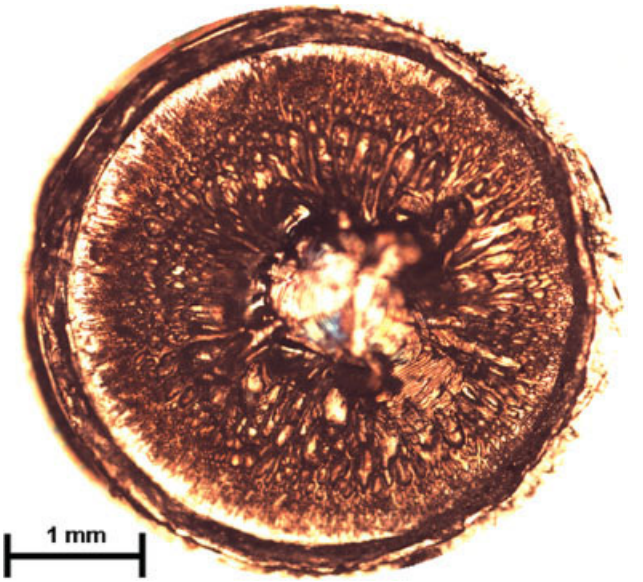

Figure 6 Optical image of a control preform gate through polarized light in the transmission mode. [Color figure can be viewed in the online issue, which is available at www.interscience.wiley.com.]

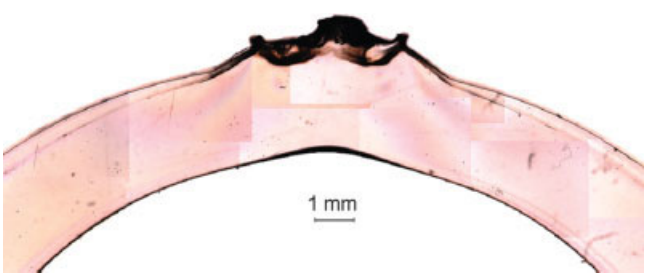

Figure 7 Optical image of a control preform in the transmission mode. [Color figure can be viewed in the online issue, which is available at www.interscience.wiley.com.]

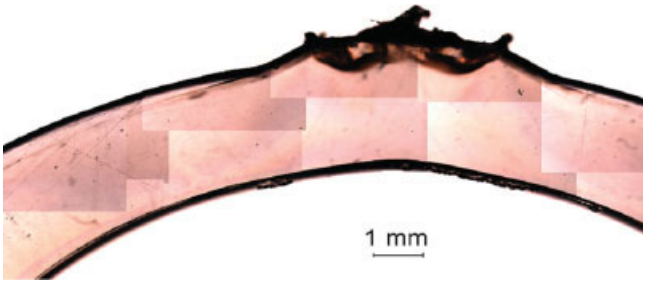

Figure 8 Optical image of an overpacked preform in the transmission mode. [Color figure can be viewed in the online issue, which is available at www.interscience.wiley.com.]

deliberate overpacking of the preforms had little effect on the bottles produced. This is a good result for bottle manufacturers as it indicates that overpacking to this degree is no restriction to producing good bottles, and generally the process is robust as far as overpacking is concerned.

Optical microscopy was used to help describe the features observed in the SAXS patterns. All optical images were recorded in the transmission mode. The samples were reasonably thick for optical microscopy, so crystalline sections appear dark with respect to amorphous regions. Figure 6 is an image of a control preform gate viewed along the long axis of the preform. The image shows that the gate is largely crystalline, with a region in the center that is less crystalline. This evidence clearly supports the SAXS results regarding the presence of oriented lamellae; however, low-magnification optical images are unable to provide any information about the lamellar alignment.

Figures 7 and 8 show combined sets of optical images taken from the control and overpacked preform U-sections, respectively. Because of the thickness of the samples, some features, particularly those around the very top of the gate, are out of focus. The preform edges in Figure 8 are also thicker than those in Figure 7, most likely as a result of the cutting and abrading process. The preform separates from the mold, leaving two corner edges on either side of the gate with an elevated nipple in the center. These often appear very dark as they may be crystalline but also somewhat out of focus with respect to the top face of the U-section. Still within the gate region, but in the body of the preform, are two dark V-shaped regions located on either side of the central channel into the mold. These regions appear to form part of the crystalline ring that can be seen clearly in Figure 6 around the center of the gate. These regions result in the off-vertical axis SAXS lobes discussed earlier. The central region of the gate, below the nipple, is observed to be less crystalline than the V-shaped regions on either side. This was also reflected in the less intense scatter observed in the SAXS patterns.

A thin crystalline layer connects to each corner of the gate and V-section and tracks the outer surface of the preform, forming a layer between the amorphous quenched skin (in direct contact with the mold) and the rest of the amorphous center. We suggest that this crystalline layer forms because of the high shear resulting from the stationary quenched layer adjacent to the mold and the main flow of material into the mold. A dark crystalline layer is also present on the inner curved surface of the preforms. All the optical images for both sets of samples follow these trends, with no major differences between the control and overpacked samples.

A possible mechanism for describing the orientation of the crystalline zones seen on either side of the central channel in the preform gate region is presented in Figure 9. During the injection-molding process, the gate valve closes after the hold phase is complete and forces a little more material into the

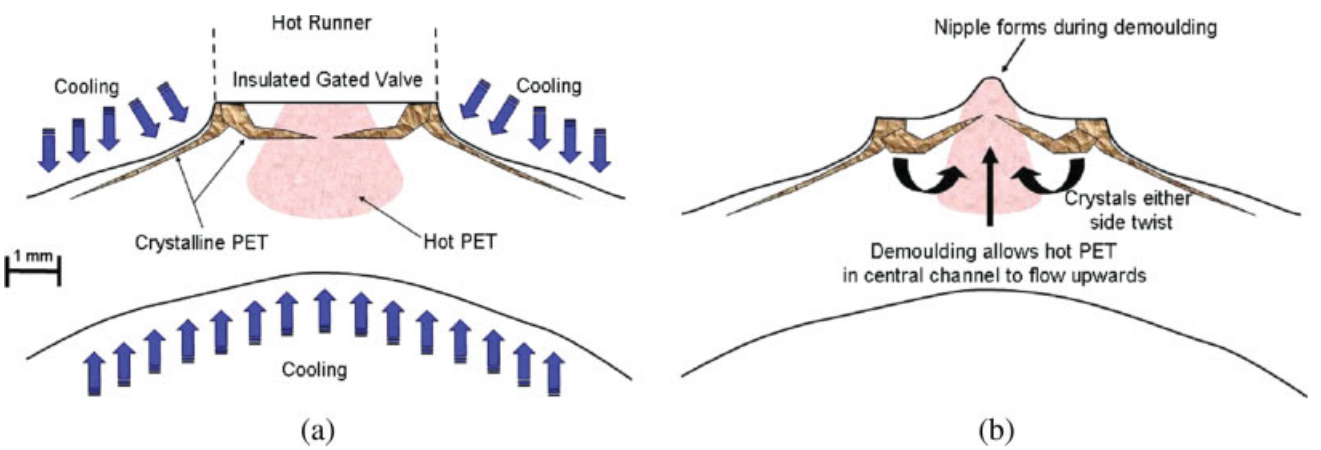

Figure 9 Schematics showing (a) the preform gate region during molding and (b) the same region shortly after demolding. [Color figure can be viewed in the online issue, which is available at www.interscience.wiley.com.]

mold, and Figure 9(a) is a schematic representing the environment after closure of the valve. Cooling is applied to the walls of the mold; however, around the gate region, cooling is less efficient because of the presence of the gate and the hot runner. As the melt flows into the mold, the polymer chains become aligned because of the high shear environment. Although short chains are able to relax quickly, long chains take much longer to relax because of entanglements. This long-lived chain alignment, coupled with the slowly cooling temperature, serves to nucleate crystallization, with lamellae forming perpendicularly to the flow direction from a sea of hot melt. Demolding removes the force holding the gate closed, and the hot central channel is able to relax, with backflow causing the nipple shown in Figure 9(b). This backflow [shown traveling upward in Fig. 9(b)] causes the newly forming crystals in the regions surrounding the central channel to twist, shifting the alignment of the lamellae off the horizontal axis and the scattered lobes off the vertical axis, as presented in the experimental SAXS patterns in Figures 2–4. This type of mechanism also explains the V-shaped features observed in Figures 7 and 8 and also why the depth of crystallites is slightly less in the central channel of Figure 4. Clearly increasing the cooling time in the mold would reduce the degree of backflow but may not offer any process advantages while incurring a penalty of reduced output. It is also important to note that the depth of the crystalline region around the gate for these samples is well within the accepted industrial tolerances.[30]

CONCLUSIONS

SAXS experiments were conducted to study the molecular morphology of control and overpacked preforms and their corresponding bottles. The preform U-sections for both sets of samples showed a highly oriented crystalline region around the gate. The orientation of the lamellae, as shown by the scattered X-rays (lobes), shifted off the axis between the central channel leading into the mold and the gate wall. The central channel was oriented but slightly less crystalline than the regions immediately on either side. The large shear forces in the gate region probably led to a high nucleation rate. The main body of the control preform was amorphous, and although the overpacked preform was mostly amorphous, it did show some evidence for weak crystallinity and orientation when the contrast of the SAXS patterns was enhanced. The scans across both sets of bottles produced very similar results, indicating that both sets of preforms produced good bottles and implying that the production process was robust to this level of preform overpacking.

Optical microscopy was conducted to support the SAXS results and produced detailed images of the crystalline regions in the U-sections. These images identified crystalline layers next to the amorphous skin layers on both the inner and outer surfaces of the preforms. The images also identified a distinctive crystalline region in the gate area of the preforms, and a model was presented to describe these. The optical images for both sets of preforms looked very similar, again implying that the process is not very sensitive to this degree of preform overpacking.

To explore these findings further, a study of the polymer chain crystallinity using wide-angle X-ray scattering was subsequently undertaken, and the results will be reported in a separate publication.[31]

The authors thank Kelvin Davies, Ron Blacker, and David Wheller for their constructive comments and for the preforms and bottles. The use of ChemMatCARS Sector 15 at the Advanced Photon Source was supported by the Australian Synchrotron Research Program, which is funded by the Commonwealth of Australia under the Major National Research Facilities Program. ChemMatCARS Sector 15 is principally supported by the National Science Foundation/Department of Energy and by the Illinois Board of Higher Education. The Advanced Photon Source is supported by the U.S. Department of Energy (through Basic Energy Sciences, Office of Science).

References

1. Cakmak, M.; Spruielli, J. E.; White, J. L. Polym Eng Sci 1984, 24, 1390.
2. Cakmak, M.; White, J. L.; Spruielli, J. E. J Appl Polym Sci 1985, 30, 3679.
3. Venkateswaran, G.; Cameron, M. R.; Jabarin, S. A. Adv Polym Technol 1998, 17, 237.
4. Ashford, E.; Bachmann, M. A.; Jones, D. P.; Mackerron, D. H. Trans Inst Chem Eng 2000, 78, 33.
5. Chevalier, L. Plast Rubber Compos 1999, 28, 385.
6. Chevalier, L.; Linhone, C.; Regnier, G. Plast Rubber Compos 1999, 28, 393.
7. Lu, W.; Debelak, K. A.; Witt, A. R.; Yang, C.; Collins, W. E.; Lott, C. J Polym Sci Part B: Polym Phys 2002, 40, 245.
8. Moldflow. http://www.moldflow.com (accessed December 12, 2006).
9. Lyu, M.-Y.; Pae, Y. J Appl Polym Sci 2003, 88, 1145.
10. Brooks, D. W.; Giles, G. A. PET Packaging Technology; Academic: Sheffield, England, 2002.
11. Hanley, T. L.; Forsythe, J. S.; Sutton, D.; Moad, G.; Burford, R. P.; Knott, R. B. Polym Int 2006, 55, 1435.
12. Hanley, T. L.; Sutton, D.; Kozior, E.; Cookson, D.; Knott, R. B. J Appl Polym Sci 2006, 99, 3328.
13. Wang, Z. G.; Hsiao, B. S.; Sauer, B. B.; Kampert, W. G. Polymer 1999, 40, 4615.
14. Hsiao, B. S.; Verma, R. K. J Synchrotron Radiat 1998, 5, 23.
15. Xia, Z.; Sue, H. J.; Wang, Z. G.; Avila-Orta, C. A.; Hsiao, B. S. J Macromol Sci Phys 2001, 40, 625.
16. Wang, Z. G.; Hsiao, B. S.; Fu, B. X.; Liu, L.; Yeh, F.; Sauer, B. B.; Chang, H.; Schultz, J. M. Polymer 2000, 41, 1791.
17. Lee, B.; Shin, T. J.; Lee, S. W.; Yoon, J.; Kim, J.; Ree, M. Macromolecules 2004, 37, 4174.
18. Lee, B.; Shin, T. J.; Lee, S. W.; Yoon, J.; Kim, J.; Youn, H. S.; Ree, M. Polymer 2003, 44, 2509.

19. Balta Calleja, F. J.; Garcia Gutierrez, M. C.; Rueda, D. R.; Piccarolo, S. Polymer 2000, 41, 4143.
20. Ezquerra, T. A.; Sics, I.; Nogales, A.; Denchev, Z.; Balta Calleja, F. J. Europhys Lett 2002, 59, 417.
21. Kiflie, Z.; Piccarolo, S.; Brucato, V.; Balta Calleja, F. J. Polymer 2002, 43, 4487.
22. Haubruge, H. G.; Jonas, A. M.; Legras, R. Macromolecules 2004, 37, 126.
23. Sutton, D.; Wanrooij, P.; Hanley, T.; Burford, R.; Heeley, E.; Knott, R. J Macromol Sci Phys 2005, 44, 1.
24. Lyu, M. Y.; Kim, H. C.; Lee, J. S.; Shin, H. C.; Pae, Y. Int Polym Process 2001, 16, 72.
25. Lyu, M. Y.; Kim, Y. H. Int Polym Process 2002, 17, 279.
26. Everall, N.; MacKerron, D.; Winter, D. Polymer 2002, 43, 4217.
27. Cookson, D.; Kirby, N.; Knott, R.; Lee, M.; Schultz, D.; Viccaro, J. J Synchrotron Radiat 2006, 13, 440.
28. Sutton, D.; Hanley, T.; Knott, R.; Cookson, D. J Synchrotron Radiat 2004, 11, 505.
29. Seki, M.; Thurman, D. W.; Oberhauser, J. P.; Kornfield, J. A. Macromolecules 2002, 35, 2583.
30. Husky Injection Molding Systems: Husky Preform Mold and System Testing Acceptance Criteria; Husky Injection Moulding Systems, Ltd.: Bolton, Canada, 2004.
31. Karatchevtseva, I.; Hanley, T.; Sutton, D.; Burford, R. P.; Cookson, D.; Knott, R. B., to appear.